ORIENTAL JOURNAL OF CHEMISTRY
An International Open Access, Peer Reviewed Research Journal
www.orientjchem.org
ISSN: 0970-020 X
CODEN: OJCHEG
2025, Vol. 41, No.(2):
Pg. 641-646

Tailoring Eu^{2+} Doped $Ba_5Al_2O_8$ Phosphors for Solid-State Lighting

SHASHI B PANDEY[1]*, APARNA J NADGAWDA[2] and CHITRA S KHADE[3]

*[1,2,3]Department of Physics, G H Raisoni University, Amravati, Maharashtra, India.
*Corresponding author E-mail: shashib.pandey@raisoni.net

http://dx.doi.org/10.13005/ojc/410233

(Received: January 08, 2025; Accepted: March 17, 2025)

ABSTRACT

Rare earth Eu^{2+} doped $Ba_5Al_2O_8$ phosphors with different concentrations of dopant were synthesized using a microwave assisted Solid state metathesis (SSM) process. Along with the structure, surface morphology its photoluminescence (PL) characteristics were studied. Eu^{2+} emission in $Ba_5Al_2O_8$ lattice was observed at 496 nm which lies in Bluish green color wavelength range of the spectrum, when it is excited at 354 nm. The emission of bluish green color is because of the Eu^{2+} ions moves from $4f^6$ 5d to $4f^7$.The presented phosphor has band gap energy E_g = 2.50eV. The maximum peak for PL intensity was obtained for a 1 mol% concentration of Eu^{2+} in $Ba_5Al_2O_8$ host lattice. The results indicated that the material could be a strong contender as a bluish green-emitting phosphor it could be promising phosphor materials can be used for solid state lighting and in the modern display systems. As it is known that the w-LEDs (white light-emitting diodes) uses Red, Green, and Blue emitting phosphors and they are the next generations lighting system and this can also be used for PDP (plasma display panel) application. The described phosphor can serve as a source for bluish-green light-emitting LEDs, enabling the fine-tuning of light spectra to optimize plant growth in controlled environment agriculture.

Keywords: Eu^{2+}, Photoluminescence, Solid state metathesis reaction, X-ray diffraction, SSL, White light emitting diode.

INTRODUCTION

With the fast expansion of modern civilization, the long-term development of energy and environmental concerns has got a lot of attention and has become a major concern for today's society. As everyone knows, lighting electricity accounts for a significant portion of total power usage in people's everyday lives and work. Traditional fluorescent and incandescent lamps, on the other hand, have a number of drawbacks related to Power consumption, efficiency to convert the energy provided, durability and environmental pollution caused[1-3]. Past 4-5 years, the industrial persons and researchers were fascinated by rare-earth ions doped luminescent materials, as these materials have several applications in variety of industries, including fiber amplifiers, solid-state illumination that includes light-emitting diodes (LEDs), medical diagnostics, biological imaging, solar cells and many more[4-7]. White LEDs (WLEDs) have been extensively used in lighting sector as a new form of solid luminescent material due to its outstanding luminescent properties, like having outstanding fluorescence efficiency, effective energy conservation, low weight, extended lifespan, less heating effect and eco friendliness. As the next generation solid-state

optical source, WLEDs are increasingly replacing traditional incandescent bulbs[8,9].

In recent years, light emitting diodes have largely superseded all types of lights and display devices. Combining a blue color light emitting light emitting diode with a cerium doped yttrium aluminium (YAG:Ce) phosphor was the first practically created white LEDs.

Phosphors in older flat panel displays and fluorescent lights were sulfur-based but prone to decay under high currents. In contrast, phosphors that are oxides and rare earth doped, offer higher thermal stability along with the chemical stability. These properties, along with high brightness and tunable emissions, have made them desirable for modern applications. Aluminate-based phosphors doped with Ce^{3+} or Eu^{2+} stand out for their durability, low toxicity, and versatile uses in LEDs, X-ray imaging, and digital displays, employing the efficient 4f-5d transitions for luminescence[10-16].

The quality of luminous material depends on many factors some of them are the precursors used, dopant used and also depends on the synthesis method used. For the production of phosphorescence materials, traditional methods some of them are solid-state reaction, combustion and sol–gel approach have inherent drawbacks like they require very high temperature and a lengthy processing time[17]. The solid state metathesis synthesis assisted with microwave approach, on the other hand, is quite straightforward. Furthermore, the SSM synthesis has several advantages. Solvent less self-propagating solid-state reactions, thus this make sure the production of a enormous variety of ceramic materials in a small span of time. These rapid solid-state metathesis reactions uses the reaction enthalpy that is released during a specific reaction. As a by-product of the SSM process, a salt having very high lattice energy was generated, which serves as the process's driving power. It is both energy-efficient and safe. A alternative source microwave oven is been used to start the reactions. Many materials like borides, metal oxides, chalcogenides and carbides synthesized via SSM processes, which are now widely acknowledged in the scientific community. Microwave radiation has been acknowledged as a practical and straightforward means to synthesis compounds since it is quicker, more cheap, and cleaner As a result, the SSM approach is a viable method for producing complicated oxide ceramics like aluminates.

We synthesized Eu^{2+} doped $Ba_5Al_2O_8$ phosphors utilizing SSM synthesis. The structural property (XRD), morphology and photoluminescence (PL) properties were analyzed. The concentration quenching, behaviour Eu^{2+} luminescence in $Ba_5Al_2O_8$ hosts is described in this work.

EXPERIMENTAL

Samples of $Ba_5Al_2O_8:xEu^{2+}$ (x = 0.1, 0.2, 0.5, 1.0 mol%) were synthesized through a microwave-assisted metathesis solid-state reaction method. The primary components include Eu_2O_3 (99.99 percent), Barium carbonate ($BaCO_3$) (99% purity, Loba chemical ltd.) and Aluminum oxide (Al_2O_3) (99% pure, Merck lab.), with small amount of activated carbon. All the reagents used were of the analytical grade. They are taken with a proper stoichiometric ratio in a pestle mortar. After mixing the sample rigorously by using mortar and pestle, the obtained paste is transferred into the silica crucible. Then kept the sample in the form of powder inside the microwave oven for 20 min at 1100K.Then the obtained powder was thoroughly washed repeatedly with deionized water and ethanol to remove the impurities, then dried overnight in an oven at 90°C. The following reaction was carried out in the synthesis process .

$$5BaCO_3 + Al_2O_3 \xrightarrow{\text{Microwave}} Ba_5Al_2O_8 + 5CO_2$$

Finally, harvest $Ba_5Al_2O_8:Eu^{2+}$ samples were collected for further analysis and discussion.

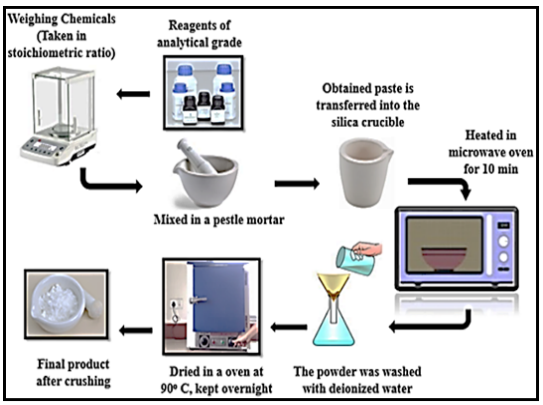

Fig. 1. Schematic diagram of synthesis of $Ba_5Al_2O_8:xEu^{2+}$

RESULTS AND DISCUSSION

Structural Analysis

The phase verification, structural parameters, and crystalline structure of $Ba_5Al_2O_8$ phosphor were thoroughly analyzed using Rigaku Miniflex-II benchtop X-ray diffractometer. The readings were taken employing Cu Kα radiation (wavelength 1.540 Å) under operating conditions of 30 kV and 15 mA, covering a 2θ range from 10° to 80°, prepared by microwave assisted solid state metathesis method. All of the detected peaks match ICDD data file Nos. 73-0202 perfectly. The obtained XRD indicates that the as prepared material is having high-purity and crystalline. Matching of the XRD patterns and absence of any extra line indicates that the desired compound is formed in phase pure manner. According to XRD readings $Ba_5Al_2O_8$ has a hexagonal structure with space group P6322. Table 1 presents the calculated d-spacing and corresponding hkl planes based on the observed 2θ values. The indexed peaks, derived from the experimental data, highlight the significant planes contributing to the diffraction pattern. The addition of Eu^{2+} to the XRD patterns has no discernible impact.

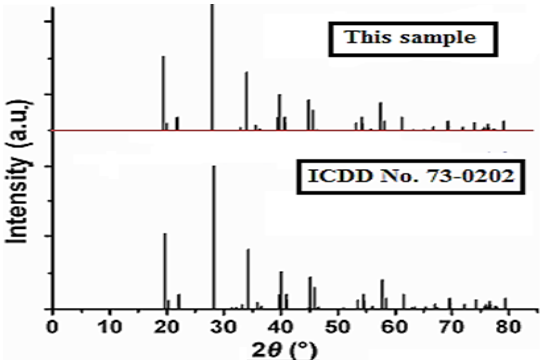

Fig. 2. XRD pattern of $Ba_5Al_2O_8$

Figure 2: XRD pattern of $Ba_5Al_2O_8$

2θ values	θ(P)	d-Spacing (Å)	hkl
19.80	9.90	4.480	(0,1,0)
20.00	10.00	4.436	(0,1,0)
22.72	11.36	3.911	(0,0,2)
28.00	14.00	3.184	(0,1,2)
34.04	17.02	2.632	(0,0,3)
40.00	20.00	2.252	(0,1,3)
45.00	22.50	2.013	(0,0,4)
57.60	28.80	1.599	(1,2,1)

Eu^{2+} luminescence

The Shimadzu RF-5301PC Spectrofluoro-photometer was used to study the excitation and emission spectrum of the present samples. The excitation spectrum of $Ba_5Al_2O_8$:Eu^{2+} is obtained for 496 nm emission wavelength , can be seen in Fig. 3(a) which has a peak at 354 nm. The $4f^7$-$4f^65d$ transition of Eu^{2+} is attributed to the excitation spectrum.

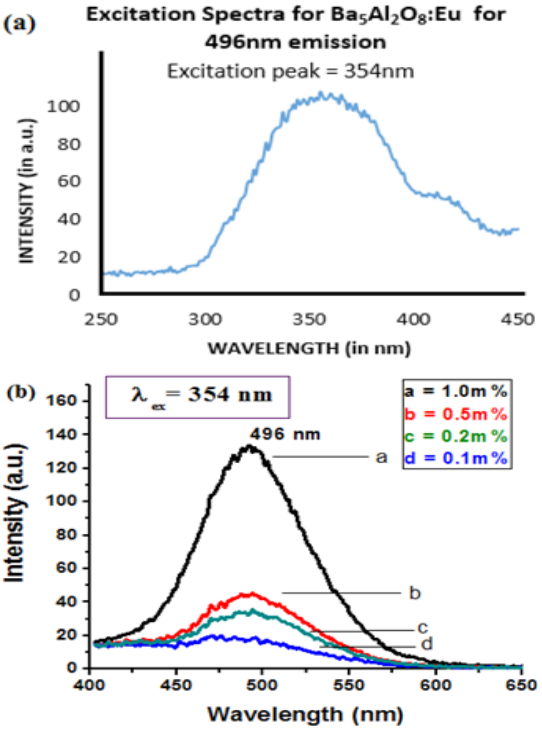

Fig. 3. Excitation Spectra (a) and Emission Spectra for $Ba_5Al_2O_8$:Eu^{2+} (b)

The emission spectra of the Eu^{2+} concentration x upon 354 nm UV irradiation are shown in Fig. 3(b) and it is observe that the profiles of emission spectra are showing almost similar pattern as the concentration of Eu^{2+} ion is increased.

The luminescence of Eu^{2+}-doped $Ba_5Al_2O_8$ phosphor arises from the electronic transitions within the Eu^{2+} ion. The excitation spectrum exhibits a prominent absorption peak at 354 nm, corresponding to the $4f^7 \rightarrow 4f^6$ 5d electronic transition of Eu^{2+}. Upon excitation, the excited electrons in the 5d state of Eu^{2+} relax to the 4f ground state, emitting photons in the visible spectrum with an emission peak at 496 nm, which corresponds to the $4f^6$ 5d $\rightarrow 4f^7$ transition[18].

The luminescence properties are influenced by the crystal field environment of the Eu^{2+} ion. In $Ba_5Al_2O_8$, Eu^{2+} substitutes for Ba^{2+}θin the host lattice. The coordination environment and

crystal field splitting affect the energy levels of the 5d orbitals, leading to variations in the emission characteristics. The host lattice's low phonon energy helps minimize non-radiative losses, enhancing luminescence efficiency[19].

Furthermore, the emission intensity of Eu^{2+} grew until it reached upto a maximum value of intensity at a Eu^{2+} concentration of 1.0m% as shown in Fig. 4(a), after which it began to decline with increasing concentration. The emission intensity dropped sharply after the critical point, owing to the concentration quenching effect. It is predicted that the energy transfer among Eu^{2+} ions is to mostly result in concentration quenching, with the possibility of this increase with increasing doping Eu^{2+} concentration until the energy is used. The emission spectrum shows bluish green color luminescence with a peak centered at 496 nm. The emission spectrum is due to $4f^65d\text{-}4f^7$ transition of dopant ion. The findings reported in the literature[20,21,22] closely align with the observed photoluminescence (PL) spectra. The emission spectra helps to determine the energy band gap of $Ba_5Al_2O_8:Eu^{2+}$ and is obtained as 2.50 eV.

The photoluminescence of as prepared $Ba_5Al_2O_8:Eu^{2+}$ is compared with the well-known phosphors YAG:Ce^{3+} used in white LEDs, such as YAG:Ce^{3+}. It is observed that YAG:Ce^{3+} emits 550 nm wavelength in the yellow region, making it suitable for blue-pumped white LEDs, while $Ba_5Al_2O_8$: Eu^{2+} offers a bluish-green emission having wavelength 496 nm, which can be useful for color tuning in white LED applications.

This bluish-green emission can be also useful in display applications where color mixing is essential to achieving high-quality white light.

The CIE chromaticity diagram of $Ba_5Al_2O_8:0.8Eu^{2+}$ shown in Fig. 4(b) obtained by using sciapps.sci-sim.com/CIE1931 indicates that the prepared phosphor exhibits bluish-green emission, showing promising research potential and can be used for green component in w-LEDs. The coordinates are given in Table 2.

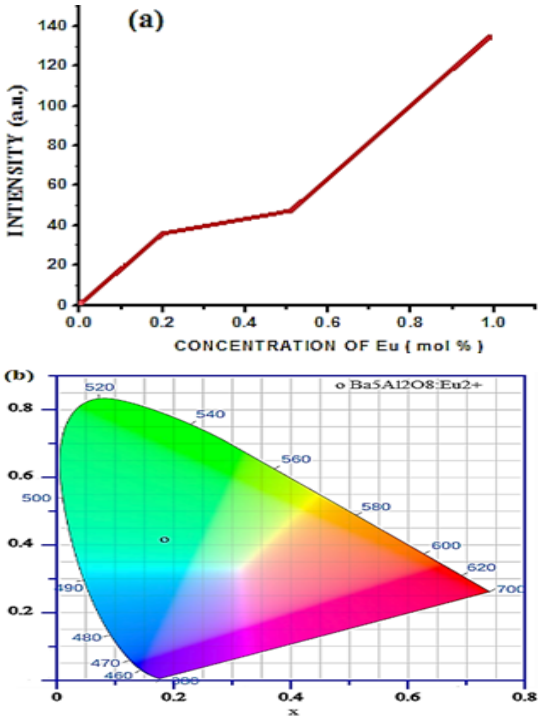

Fig. 4. Graph of emission intensity verses concentration x in $Ba_5Al_2O_8:xEu^{2+}$ (a) and the CIE chromaticity diagram of $Ba_5Al_2O_8:0.8Eu^{2+}$ (b)

Table 2: CIE chromaticity coordinates for $Ba_5Al_2O_8:0.8Eu^{2+}$

Phosphor	CIE chromaticity coordinates		Color
	x-coordinate	y-coordinate	
$Ba_5Al_2O_8:0.8Eu^{2+}$	0.185	0.416	Bluish-Green

Surface morphology

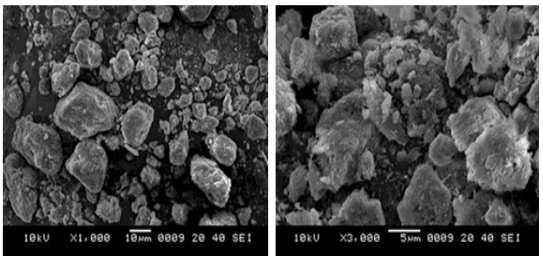

Fig. 5. SEM image of $Ba_5Al_2O_8:Eu^{2+}$

Additionally,the surface morphology (Fig. 5) shows particles have a tendency to accumulate creating small masses having non-uniform as well as different sizes and shapes which is obtained by using JEOL (JSM-6380) scanning electron microscope. The phosphors display irregular morphologies, with diameters ranging from 2 to 20 µm. There are some spherical structures having fissures and pores. Many pores are observed is

due to the release of large amount of gases during synthesis process. The variation in crystalline sizes, characterized by sharp boundaries and irregular particle shapes, can be attributed to the uneven distribution of temperature and mass flow during the synthesis process. This is distinctly visible in Fig. 5, with a resolution reaching up to 5 µm.

The high thermal stability of $Ba_5Al_2O_8:Eu^{2+}$ is also influenced by the covalent nature of the bonding in the host lattice. The presence of Al–O bonds contributes to the rigidity of the structure, reducing lattice distortions under high temperatures and thereby minimizing thermal quenching[23]. Unlike sulfide-based phosphors that degrade over time due to oxidation and moisture sensitivity, $Ba_5Al_2O_8:Eu^{2+}$ demonstrates excellent chemical stability, making it more suitable for long-term applications.

Occupancy of Eu^{2+} at different crystallographic sites from emission wavelength

We utilized Van Uitert's empirical formula[21,22] to explore the link between emission wavelength and the sites of Ba^{2+} which are occupied by Eu^{2+}. Van Uitert used the following empirical formula to compute the locations of Eu^{2+} ions that are in the lower d-band:

$$E = Q\left[1 - \left(\frac{V}{4}\right)^{1/V} 10^{\frac{-n.ea.r}{80}}\right] \quad (1)$$

Where E is energy edge of lower d-band for Eu^{2+} ions in 3D structure, Q is the energy edge of the lower d-band (for the as prepared sample doped with Eu^{2+} ion Q = 34000 cm^{-1}), V is the valence of the active cation (here V is +2 for Eu^{2+}), where n denotes the number of anions in the immediate shell around this ion, ea denotes the coordination radial's electron affinity, and r is the radius of the host cation replaced by the activator. r is 1.47 eV and ea is 1.60 eV in $Ba_5Al_2O_8$ for Ba^{2+} ions. Eq. (1) yields 20930 cm^{-1} (496 nm) for Eu^{2+} as the estimated values of E. The Eu^{2+} doped $Ba_5Al_2O_8$ emission peaks are detected at 20161.29 cm^{-1} (496 nm), shown in Fig. 3. This demonstrates that theoretical and experimental values are extremely well aligned. Eu^{2+} occupy the Ba^{2+} position in $Ba_5Al_2O_8$ as a result.

CONCLUSION

A microwave aided solid state metathesis reaction technique has been used to effectively produce Eu^{2+} doped $Ba_5Al_2O_8$ phosphor. The hexagonal structure of $Ba_5Al_2O_8$ with space group $P6_322$ was verified by XRD patterns for produced phosphors. The emission peaks of Eu^{2+} doped $Ba_5Al_2O_8$ phosphors in PL properties are 496 nm for 0.1, 0.2, 0.5, and 1.0 m%, respectively. In Eu^{2+} doped $Ba_5Al_2O_8$ phosphor, concentration quenching occurred at concentrations greater than 1m%. The energy band gap of $Ba_5Al_2O_8:Eu^{2+}$ is obtained as 2.50 eV. All of the tests demonstrate that this phosphor can be a bluish green phosphor with research potential and can be a candidate for green component in w-LEDs.

The unique bluish-green luminescence of $Ba_5Al_2O_8:Eu^{2+}$, coupled with its superior thermal stability, high quantum efficiency, and robust structural integrity, makes it a promising candidate for next-generation white LEDs.

And this Bluish-green color-emitting LEDs enhance controlled environment agriculture by fine-tuning light spectra for optimized plant growth and photosynthesis, promoting compact, healthy crops while improving energy efficiency in indoor farming systems.

Funding Sources

The author(s) received no financial support for the research, authorship, and/or publication of this article.

Conflict of Interest

The author(s) do not have any conflict of interest.

REFERENCES

1. Pattison, P.; Tsao, J.; Brainard, G.; Bugbee, B., *Nature.*, **2018**, *563*, 493–500.
2. Xia, Z. G.; Liu, Q. L., *Prog. Mater. Sci.*, **2016**, *84*, 59–117.
3. Saidi, K.; Dammak, M., *RSC Adv.*, **2020**, *10*, 21867–21875.
4. Schubert, E. F.; Kim, J. K., *Science.*, **2005**, *308*, 1274–1278.
5. Push, P.; Schmidt, P. J.; Schnick, W., *Nat. Mater.*, **2015**, *14*, 454.
6. Xia, Z.; Meijerink, A., *Chem. Soc. Rev.*, **2017**, *46*, 275–299.

7. Guo, H.; Zheng, Z.G.; Teng, L.M.; Wei, R.F.; Hu, F.F., *J. Lumin.*, **2019**, *213*, 494–503.
8. Wang, L.; Xie, R. J.; Suehiro, T.; Takeda, T.; and Hirosaki, N., *Chem. Rev.*, **2018**, *118*, 1951–2009.
9. Kang, F. W.; Sun, G. H.; Boutinaud, P.; Gao, F.; Wang, Z. H.; Lu, J.; Li, Y. Y.; Xiao, S. S., *J. Mater. Chem.* C., **2019**, *7*, 11041.
10. Jüstel, T.; Nikol, H.; Ronda, C., *Angew Chem Int Edit.*, **1998**, *37*, 3084–3103.
11. Zheng, Y.; Chen, D., *Luminescence.*, **2011**, *26*, 481–485.
12. Salah, N.; Habib, S.S.; Khan, Z.H., *J Fluoresc.,* **2010**, *20*, 1009–1015.
13. Blasse, G.; Wanmaker, W.L.; Ter Vrugt, J.W., *Philips Res Rep.,* **1968**, *23*, 189–200.
14. Yamazaki, K.; Nakabayashi, H.; Kotera, Y., *J Electrochem Soc.*, **1986**, *133*, 657–660.
15. Mothudi, B.M.; Ntwaeaborwa, O.M.; Botha, J.R., *Physica* B., **2009**, *404*, 4440–4444.
16. Palilla, F.C.; Levine, A.K.; Tomkus, M.R., *J Electrochem Soc.*, **1968**, *115*, 642–644.
17. Lou, Z.; Hao, J.; Cocivera, M., *J Phys D:Appl Phys.*, **2002**, *35*, 2841–2845.
18. Blasse, G.; Grabmaier, B. C.; Luminescent Materials., **1994**.
19. Van Uitert, L. G., *Journal of the Electrochemical Society.*, **1967**, *114*(10), 1048-1052.
20. Lin, Y.; Zhang, Z.; Tang, Z., *Mater Chem Phys.,* **2001**, *70*, 156–159.
21. George, N. C., Denault, K. A., & Seshadri, R. Phosphors for solid-state white lighting., *Annual Review of Materials Research*, **2013**, *43*, 481-501. https://doi.org/10.1146/annurev-matsci-071312-121656
22. Van Uitert, L.G., *J Lumin.*, **1984**, *29*, 1–9.
23. Kai Li.; Mengjiao Xu, Jian Fan., *J. Mater. Chem.* C., **2015**, 00, 1-9.
24. George, N. C.; Denault, K. A.; Seshadri, R., *Annual Review of Materials Research.,* **2013**, *43*, 481-501.